1. Przemysław SOBKIEWICZ[1]

Politechnika Wrocławska, Wydział Informatyki i Telekomunikacji, Katedra Telekomunikacji i Teleinformatyki (1)

doi:10.15199/48.2024.06.31

Split Ring Resonator Based Probe for Detection of Subsurface Defects in Composite Materials

Streszczenie. *Rozdzielczość obrazowania konwencjonalnych sond pola bliskiego jest ściśle związana z rozmiarami jej apertury. Osiągnięcie wysokiej rozdzielczości obrazu najczęściej wymaga operowania na bardzo wysokich częstotliwościach. W niniejszej pracy przedstawiono sondy oparte o struktury dzielonych rezonatorów pierścieniowych, które odpowiednio wykorzystane zapewniają wysoką rozdzielczość i czułość przy zachowaniu niskiego pasma pracy. Prace wykonano na przykładzie detekcji wad podpowierzchniowych w materiale kompozytowym – fragment zbiornika (GFRP) do przechowywania wodoru.*

Abstract*. The imaging resolution of conventional near-field probes is often limited to dimensions of an aperture. To achieve imaging resolution in the order of few millimeters using standard aperture probes it is required to operate at very high frequencies. In contrast, planar structure based on Split Ring Resonator (SRR) could provide high resolution and sensitivity while working at low frequency range. This paper proposes an high-sensitivity SRR-based microwave sensor for detection of common undersurface flaws in composite-made samples (GFRP) of tank for hydrogen storage. (**Dzielony rezonator pierścieniowy jako sonda przeznaczona do detekcji podpowierzchniowych wad materiałów kompozytowych**).*

Słowa kluczowe: NDT, Obrazowanie mikrofalowe, Dzielony Rezonator Pierścieniowy, Materiał kompozytowy z włókna szklanego.
Keywords: NDT, Microwave Imaging, Split Ring Resonator, GFRP Tanks.

Introduction

Modern composite tanks have high storage pressure to weight ratio, aging and corrosion resistance. That plays an important role in manifold industrial sectors such as aviation or automotive especially in petroleum and natural gas storage and transportation systems. Due to unique properties it is a material that rapidly replace metal constructions, partially or fully. Particularly in hydrogen storage and piping systems where the trend in the use of composite materials is noticeable. Nevertheless, non-metallic composite tanks and pipes are vulnerable for defects due to manufacturing factors, strikes or long-term use in hostile environment. The long-term existence of these defects will affect the composite tank high-pressure resistance properties and increase burst possibility [1,2]. To

Microwave imaging introduces a wholesome, non-ionizing method to fill in the gaps in existing techniques such as Ultrasound, X-ray and Computed Tomography, Magnetic Resonance or Shearography [3,4].

There is a lot of significant and notable microwave imaging systems that have important applications, especially in medical imaging, ground penetrating radars or flaws detection in non-destructive testing for composite materials [3,5–8]. Recent applications of microwave NDT cover others areas like corrosion detection covered by paint [9], surface flaw detection in metallic and non-metallic materials [10–12] or delamination detection in T-joints of wind turbine [13]. Major advantages of microwave NDT technique is at least one-side access, non-contact nature, high penetration depth and no couplant medium needed.

Typically, the purpose of microwave imaging is to determine the parameter distribution over the investigated region according to scattering parameters data, using reflection (S_{11}) and/or transmission (S_{21}) methods. Each resonant frequency responds only to the defects in its own electromagnetic (EM) sensitive area, which is mainly manifested as resonant frequency shift or resonant magnitude and phase change [14].

Many types of SRR-based sensors are widely used in various imaging, NDT and NDE applications [10,11,14–16]. They are also applied for materials permittivity characterization [17,18] and moisture content evaluation [19].

Designed SRR structures are able to restrain signal propagation on narrow resonant frequency band. The whole structure EM behaviour depends on each ring dimensions, especially: width, length, asymmetry, relative distance between each ring, edge gaps and the way of coupling with transmission line. Resonant frequency shift is followed by dielectric coupling variation due to dielectric properties differences between healthy-state composite and faulty part.

Investigated SRR consists of a rectangular and circular rings. Proper geometry optimization leads to a unique resonant frequency and higher penetration depth because of low resonant frequency. A modified SRR geometry is used for composites interrogation through structure edge coupling. This paper proposes a sensor that has the advantages of high detection efficiency, relatively simple geometry. The main goal is to design a novel near-field probe based on Split Ring Resonator for microwave NDT applications. The presented analysis based on simulation model lead to determining applicability of the sensor.

SRR-based Probes Theory

SRR excited by a time-varying magnetic field behaves as a subwavelength resonator. A planar rectangular SRR behave as a simple LC resonance circuit, with the resonant frequency f_r given by equation 1 [20].

(1) $$f_r = \frac{1}{2\pi \cdot \sqrt{LC}}$$

where L and C are the effective inductance and capacitance of SRR equivalent circuit, respectively.

The transmission fed line parameters, as well as the SRR dimensions changes the overall probe inductance and capacitance and are thus responsible for affecting the resonant frequency of the entire sensor system.

The SRR structure has capacitive elements that increase the response of the material to the incident EM field. Total capacitance of the SRR system has mainly two contributions - first arising from the splits width and second from the gap between the rectangular or circular rings. The presence of splits in rings eliminates the half-wavelength requirement for resonance. However, increasing split width or shape (capacitance increase) leads to a decrease of resonant frequency [20]. In the aftermath, through accurate split width adjustment it is possible to decrease the resonant frequency without significant change in probe dimensions.

When a material under investigation is placed in close proximity to the resonator, the sensor resonant frequency is changed due to dielectric loading. Perturbation theory for a cavity resonator [21] states that a frequency shift due to the presence of a material of volume V is given by equation 2.

(2) $$\frac{\Delta f}{f_0} = -\frac{\iiint_V (\Delta\mu|H_0|^2 + \Delta\varepsilon|E_0|^2)dV}{\iiint_V (\mu|H_0|^2 + \varepsilon|E_0|^2)dV}$$

where E_0 and H_0 are the electric and magnetic field respectively, ε and μ are the basic permittivity and permeability, and Δε and Δμ are the change of material properties introduced by another dielectric material.

The frequency shift can be subsequently utilized to detect the presence of a dielectric parameters change in a sample. To enhance the dielectric loading, the tips of the outer sensing ring are added and extended along the sensor edge. Additional tips increase inductance and capacitance due to the additional metal and increase in plate area lead to decrease of SRR resonant frequency (equation 1), and it is evident from figure 2. The fields generated from the extended sensor tips are also higher than that of a conventional sensor (without tips). The fringing fields generated between the splits and edges of the conventional SRR sensor are directed towards the top surface and to the sensor edges. In order to increase the sensitivity and resolution of the sensor the samples are scanned from the edge of the sensor instead of the top surface.

Probes Design

The design of the proposed near-field probes has been done using 3D EM simulation and analysis software - Computer Simulation Technology (CST) Microwave Studio using a frequency-domain solver. Investigated frequencies range from 4 GHz (λ= 7.50 cm) to 5 GHz (λ = 6.00 cm). The work presents 2 types of resonators – ring, rectangular and their modification in the form of added tips. First pair of developed planar resonant probes consists of two rectangular rings of width w. Second pair of probes consists of two rings of diameter r1 and r2 (Figure 1). Probe dimensions with their components are presented in table 1. Each probe is fed by a transmission line. Dimensions and parameters were obtained during CST optimization procedure. FR4 substrate with relative permittivity equal to 4.3 was used, with the SRR and the feeding transmission line laid on the top layer.

Table 1. Geometry parameters of developed probes

Parameter	P1	P2	P3	P4
w1 [mm]	5.4		-	
w2 [mm]	3.2		-	
g [mm]	0.8		0.6	
r1 [mm]	-		2.0	
r2 [mm]	-		3.1	
k [mm]	0.5		0.5	
d [mm]	-	2	-	2.2

The resolution from the radiating surface of the SRR probe is typically the size-close to the SRR face footprint (sensing area). Therefore, smaller probes will yield a higher image resolution. Nevertheless, the resolution and sensitivity can be increased by optimizing the outer split ring, its gap and its overall shape to optimize coupling factor. In this case, SRR with additional tips was investigated. The simulated $|S_{21}|$ parameters for unloaded probes are shown in figure 2.

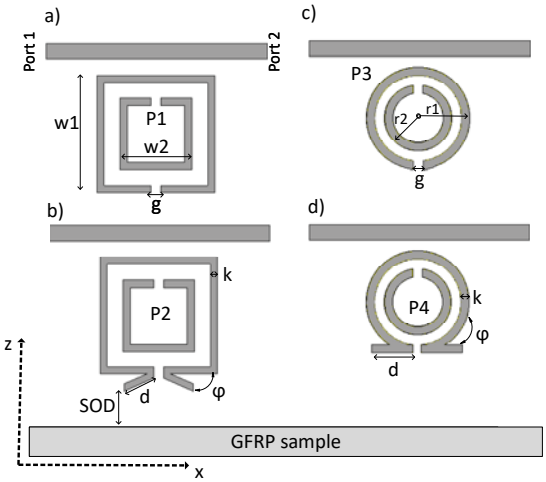

Fig. 1. Microstrip Split Ring Resonator-based near-field probe: (a) 2 rings rectangular ring SRR b) 2 rings rectangular ring SRR with tips; (c) 2 rings circular SRR d) 2 rings circular SRR with tips

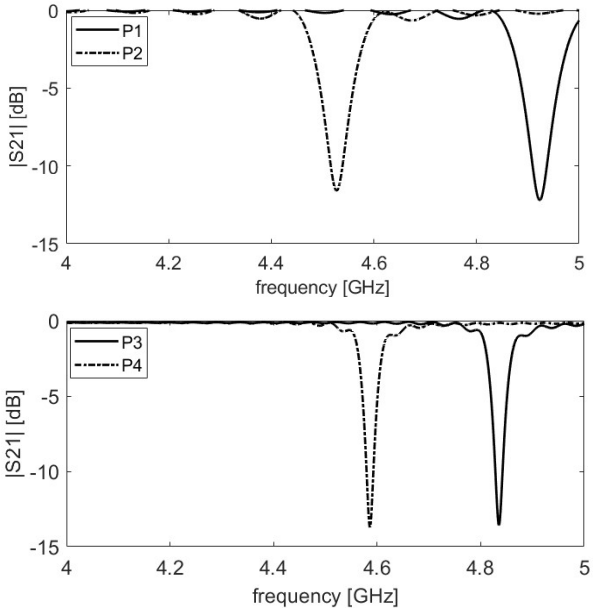

Fig. 2. The simulated magnitudes of the S_{21} coefficient as a function of frequency for investigated probes

Table 2. Geometry properties of proposed SRR-based near-field probes

Probe No.	P1	P2	P3	P4
Resonant frequency [GHz]	4.93	4.52	4.83	4.58

The fundamentals of the probe imaging attributes are based on the field distribution in the near-field region of sensing area. The effective way to improve the sensitivity is increase the electromagnetic field in the probe near-field sensing region. The radiated near-field distributions for examined probes were investigated. Figure 3 shows the normalized electric field along the x-axis at stand-off distance (SOD) z =1.0 mm from probe edge for all probes. The presented field distributions were obtained at the probes resonance frequencies. It is shown that probes with additional tips of different length (P2 and P4) provide higher field distribution along the sensing axis. It was also noticed that, as the SOD increases, the near-field diminishes at the center (x=0mm) of the field distribution.

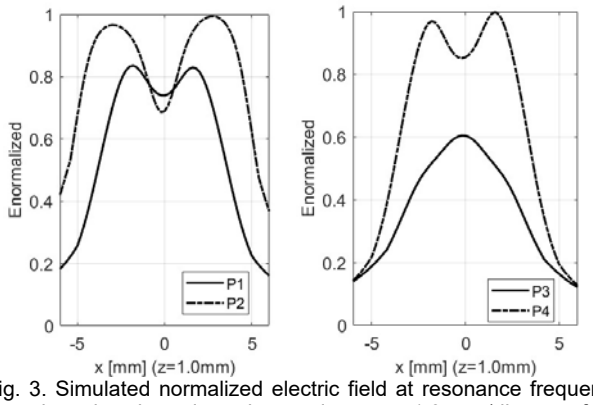

Fig. 3. Simulated normalized electric field at resonance frequency for selected probes along the x-axis at z = 1.0mm (distance from probe edge)

The resonance properties are strongly affected by SRR geometry. The results presented above show that probes 2 and especially 4 are good candidates for undersurface flaws detection. The application of the developed probes for near-field imaging and their capability to identify flaws edges were further validated by acquiring two-dimensional (2D) images of composite sample.

Simulation results

From the microwave NDT standpoint, a subsurface inclusions and defects are announced by a change in the complex dielectric constant and from the sensor point of view change of scattering parameters. The purpose of the imaging system is to catch changes and spatially map them into two or three-dimensional images. In presented simulations selected probes were evaluated for purposes of 2D imaging of composite samples.

Material Under Investigation

The composite material under test (MUT) is a part of composite tank for hydrogen storage (without internal metal liner). MUT material is a Glass Fiber Reinforced Polymer (GFRP) that consists of mixture of glass fibers and resin binder. Dielectric properties of real samples were measured using SPDR resonator and coaxial line, the relative electrical permeability of MUT is 4.6 and loss tangent (tan δ) is 0.01. The dimensions of a part under investigation are 50x50x32mm. Simulated undersurface flaws are an longitudinal lines filled with air.

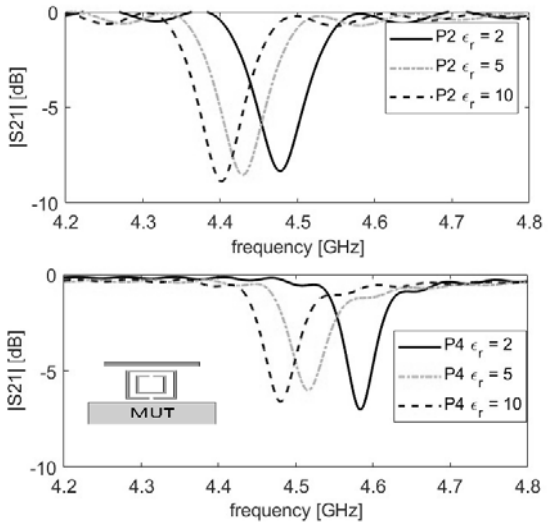

Fig. 4. $|S_{21}|$ Resonance relationship to dielectric constant of MUT

Resonant frequency of the SRR is changing due to presence of a dielectric material in close proximity. Three dielectric materials with relative dielectric constant equal to 2, 5 and 10 were placed near probe edge with SOD = 0.5mm (Fig. 4). It was shown that probes resonant frequencies shifts due to dielectric loading of a material.

Imaging Purposes of Developed Probes

Presented images were obtained during probe movement along y-axis (probe oriented by substrate width) above the GFRP sample. Flaws distribution and parameters was shown in figure 5 and Table 3, respectively. Figures 6-7 shows Δf of resonant-frequencies for each scanning spatial point. Parameter Δf is equal to a difference in resonant frequency under healthy state composite and the simulated resonant frequency in an actual probe position.

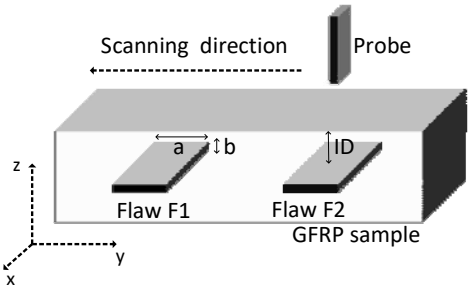

Fig. 5. Scheme of undersurface flaws arrangement in investigated GFRP composite sample

Table 3. Undersurface flaws geometry.

Parameter	F1	F2
a [mm]	10	5
b [mm]	2	2
ID [mm]	1	3

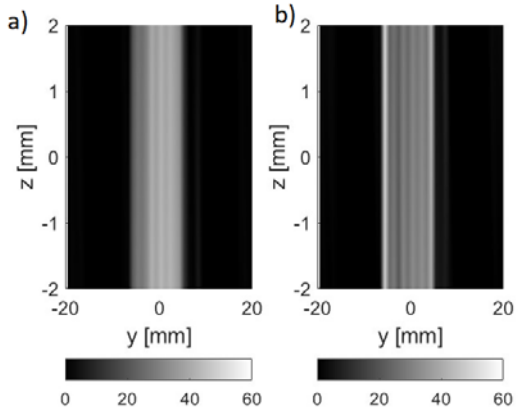

Fig. 6. Δf $|S_{21}|$ for defect F1 with SOD = 1.0 mm. a) Probe 2 b) Probe 4

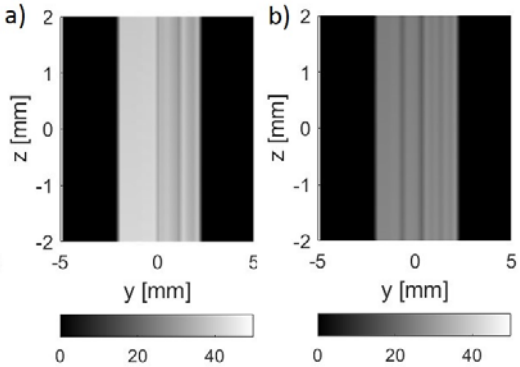

Fig. 7. Δf $|S_{21}|$ for defect F2 with SOD = 1.0 mm. a) Probe 2 b) Probe 4

Table 4. Comparison of results obtained by considered probes

Probe No.	F1 $\Delta f_{average}$ [MHz]	F2 $\Delta f_{average}$ [MHz]
P2	47	38
P4	35	27

Consequently, based on the simulation results, modified probes number 2 and 4 provide high sensitivity for undersurface defect. Investigated probes provide noticeable resonant frequency shift when facing the defect (Table 4). It is worth noticing that probes indicate orientation predispositions - higher resolution was obtained during scanning along broadside of probe rather than thin side which is mainly dictated by the near-field distribution differences.

Summary

Improved Split-Ring Resonators as a near-field imaging probes were presented. The proposed sensors structures consist of rectangular or circular rings with outer ring gap ended with additional tips. Tips significantly decrease the probe resonant frequency which consequently increases the EM penetration depth. Furthermore, according to figure 3. additional tips enhance probe sensitivity. Edge scanning reduces the coupling of the transmission line with the MUT. The simulation results prove that presented probes can improve the detection ability with high resolution remaining on relatively low frequency band. The advancement of near-field microwave imaging probes are often aimed at enhancing the sensitivity and resolution without substantial increase of complexity or implementation cost. This paper presents sensing probes design that utilize metamaterial unit cells coupled to microstrip fed line. It has been shown that the microwave split-ring resonator can be useful for imaging of GFRP structures and for detection of common undersurface defects such as delamination or inclusions. The probes provides an orientation-dependent response. Due to high sensitivity, the application of an extended SRR geometry with edge scanning can provide an improved image quality and accuracy compared to using a standard, surface oriented probes. Based on simulation results the proposed sensors resonate in frequency range 4.3–4.5 GHz while loaded by MUT. During simulation studies and parametric analysis it was noted that S_{21} magnitude and phase are also sensitive for dielectric loading and thus can be used to resonance shift determination. It was shown that even small geometry modification of outer SRR ring can improve the NDT and NDE results. Presented work is of further research aimed at extending the near-field probe development – especially improvement of resonant structure geometries.

Author: mgr inż. Przemysław Sobkiewicz**,** Politechnika Wrocławska, Wydział Informatyki i Telekomunikacji, Katedra Telekomunikacji i Teleinformatyki,
E-mail: Przemyslaw.Sobkiewicz@pwr.edu.pl

References

[1] ASM Handbook Composites; ASM International, Ed.; 10th editon.; ASM International: Materials Park, Ohio, 1990; Vol. Volume 21; ISBN 978-0-87170-377-4.
[2] Gibson, R.F. Principles of Composite Material Mechanics; Mechanical engineering : a series of textbooks and reference books; Fourth edition.; CRC Press, Taylor & Francis Group: Boca Raton, 2016; ISBN 978-1-4987-2069-4.
[3] Pastorino, M. Microwave Imaging Methods and Applications; Artech House: Boston, 2018; ISBN 978-1-63081-348-2.
[4] Zoughi, R. Microwave Non-Destructive Testing and Evaluation; Springer Netherlands: Dordrecht, 2000; ISBN 978-94-015-1303-6.
[5] Zhang, H.; Yang, R.; He, Y.; Foudazi, A.; Cheng, L.; Tian, G. A Review of Microwave Thermography Nondestructive Testing and Evaluation. Sensors 2017, 17, 1123, doi:10.3390/s17051123.
[6] Saleh, W.; Qaddoumi, N. Potential of Near-Field Microwave Imaging in Breast Cancer Detection Utilizing Tapered Rectangular Waveguide Probes. Comput. Electr. Eng. 2009, 35, 587–593, doi:10.1016/j.compeleceng.2008.08.005.
[7] Saleh, W.; Qaddoumi, N.; Abu-Khousa, M. Preliminary Investigation of Near-Field Nondestructive Testing of Carbon-Loaded Composites Using Loaded Open-Ended Waveguides. Compos. Struct. 2003, 62, 403–407, doi:10.1016/j.compstruct.2003.09.012.
[8] Malyuskin, O.; Fusco, V.F. High-Resolution Microwave Near-Field Surface Imaging Using Resonance Probes. IEEE Trans. Instrum. Meas. 2016, 65, 189–200, doi:10.1109/TIM.2015.2476277.
[9] Rahman, M.S. ur; Abou-Khousa, M.A. Millimeter Wave Imaging of Surface Defects and Corrosion under Paint Using V-Band Reflectometer. In Proceedings of the 2019 IEEE International Conference on Imaging Systems and Techniques (IST); IEEE: Abu Dhabi, United Arab Emirates, December 2019; pp. 1–5.
[10] Xie, Z.; Li, Y.; Sun, L.; Wu, W.; Cao, R.; Tao, X. A Simple High-Resolution Near-Field Probe for Microwave Non-Destructive Test and Imaging. Sensors 2020, 20, 2670, doi:10.3390/s20092670.
[11] Zhou, X.; Yang, X.; Su, P.; Wang, J.; Wang, Z.; Peng, H.; Gu, D. Detection and Location of Defects in Non-Metallic Composites Pipeline Based on Multi-Resonant Spoof Surface Plasmon Polaritons. IEEE Sens. J. 2022, 22, 2091–2098, doi:10.1109/JSEN.2021.3134986.
[12] Tiwari, N.K.; Singh, S.P.; Akhtar, M.J. Near Field Planar Microwave Probe Sensor for Nondestructive Condition Assessment of Wood Products. J. Appl. Phys. 2018, 123, 224502, doi:10.1063/1.5028259.
[13] Li, Z.; Soutis, C.; Haigh, A.; Sloan, R.; Gibson, A.; Karimian, N. Microwave Imaging for Delamination Detection in T-Joints of Wind Turbine Composite Blades. In Proceedings of the 2016 46th European Microwave Conference (EuMC); IEEE: London, United Kingdom, October 2016; pp. 1235–1238.
[14] Mayani, M.G.; Herraiz-Martinez, F.J.; Domingo, J.M.; Giannetti, R. Resonator-Based Microwave Metamaterial Sensors for Instrumentation: Survey, Classification, and Performance Comparison. IEEE Trans. Instrum. Meas. 2021, 70, 1–14, doi:10.1109/TIM.2020.3040484.
[15] Xie, Z.; Wang, G.; Sun, L.; Li, Y.; Cao, R. Localised Spoof Surface Plasmon-based Sensor for Omni-directional Cracks Detection in Metal Surfaces. IET Microw. Antennas Propag. 2019, 13, 2061–2066, doi:10.1049/iet-map.2018.5749.
[16] Malyuskin, O.; Fusco, V. Resonantly Loaded Apertures for High-resolution Near-field Surface Imaging. IET Sci. Meas. Technol. 2015, 9, 783–791, doi:10.1049/iet-smt.2014.0337.
[17] Pechrkool, T.; Sangmahamad, P.; Thiamsinsangwon, P.; Sutham, T.; Kumkhet, B.; Pirajnanchai, V. High-Sensitivity Contactless Microwave Sensor Based on Rectangular Complementary Split Ring Resonator for Glucose Concentration Characterization. In Proceedings of the 2022 37th International Technical Conference on Circuits/Systems, Computers and Communications (ITC-CSCC); IEEE: Phuket, Thailand, July 5 2022; pp. 971–974.
[18] Galindo-Romera, G.; Javier Herraiz-Martinez, F.; Gil, M.; Martinez-Martinez, J.J.; Segovia-Vargas, D. Submersible Printed Split-Ring Resonator-Based Sensor for Thin-Film Detection and Permittivity Characterization. IEEE Sens. J. 2016, 16, 3587–3596, doi:10.1109/JSEN.2016.2538086.
[19] Baghelani, M.; Hosseini, N.; Daneshmand, M. Selective Measurement of Water Content in Multivariable Biofuel Using Microstrip Split Ring Resonators. In Proceedings of the 2020 IEEE/MTT-S International Microwave Symposium (IMS); IEEE: Los Angeles, CA, USA, August 2020; pp. 225–228.
[20] Aydin, K.; Bulu, I.; Guven, K.; Kafesaki, M.; Soukoulis, C.M.; Ozbay, E. Investigation of Magnetic Resonances for Different Split-Ring Resonator Parameters and Designs. New J. Phys. 2005, 7, 168–168, doi:10.1088/1367-2630/7/1/168.
[21] Waldron, R.A. Perturbation Theory of Resonant Cavities. Proc. IEE Part C Monogr. 1960, 107, 272, doi:10.1049/pi-c.1960.0041.